

석회암층 교대 하부 구조물의 안정성 해석

최성웅¹⁾ · 김기석²⁾

Stability Analysis on the Substructure of Abutment in Limestone Basin

Sung-Oong Choi and Ki-Seog Kim

Abstract. Natural cavities were found at shallow depth during construction of a huge bridge in Cambro-Ordovician Limestone Basin in the central part of Korea. The distribution patterns of cavities in this area were investigated carefully with a supplementary field job such as a structural geological survey, a geophysical survey, and a rock mechanical test in laboratory or field. A structural geological mapping produced a detail geological map focusing the route of the proposed highway. It suggested that there were three faults in this area, and these faults had an influence on the mechanism of natural cavities. Among many kinds of geophysical surveys, an electrical resistivity prospecting was applied first on the specific area that was selected by results from the geological survey. Many evidences for cavities were disclosed from this geophysical data. Therefore, a seismic tomography was tested on the target area, which was focused by results from the electrical resistivity prospecting and was believed to have several large cavities. A distinct element numerical simulation using the UDEC was followed on the target area after completing all of field surveys. Data from field tests were directly dumped or extrapolated to numerical simulations as input data. It was verified from numerical analysis that several natural cavities underneath the foundation of the bridge should be reinforced. Based on the project result, finally, most of foundations for the bridge were re-examined and the cement grouting reinforcement was constructed on several foundations among them.

KeyWords: Geophysical Survey, Natural Cavity, Numerical Simulation, Structural Geological Mapping

초 록. 중부지역에 존재하는 대규모 석회암층을 통과하는 고속도로가 신설되는 가운데, 일부 교량의 교대 하부 얽은 심도에서 자연 생성된 석회암 공동이 다수 발견됨에 따라, 교대 및 교량의 안정성 확보를 위한 추가 정밀조사가 실시되었다. 정밀구조지질조사를 통해 고속도로 노선을 따른 지질도가 작성되었으며 이를 토대로 전기비저항 탐사가 일부 구간에 대해 실시되었다. 이 결과 석회암 공동의 존재가 의심되는 부분에 대해 국부적인 탄성파탐사가 수행됨으로써 석회암 공동의 위치 및 규모가 최종 파악되었으며, 일련의 현장조사 및 실험실 시험결과를 이용한 수치해석이 이루어졌다. 수치해석에 의한 교대 및 교량의 안정성 분석 결과, 시멘트 그라우팅에 의한 교량 하부 기초의 보강이 제안되었다.

핵심어: 석회암 공동, 구조지질조사, 전기비저항탐사, 탄성파탐사, 수치해석

1. Introduction

Recently, Korean society needs a transportation network to be more perfect and reliable with their rapid expansion in economy and industry. With these demands, basic industries such as highway or railroad are increasing their volume. The Kyung-Bu high-speed

railroad that extends to a distance of about 450 km from Seoul to Busan is a good example.

Nevertheless a transportation network in Korea mostly consists of tunnels or bridges, because about 70% of the Korean peninsular is covered in a mountainous area. More than 40% of total extensions in the Kyung-Bu high-speed railroad, for instance, are consisted of tunnels and bridges.

As for a tunnel, whatever it is a shallow one or a deep one, it has been constructed with a consortium of geologists, geophysicists, rock engineers, and civil

¹⁾정회원, 한국지질자원연구원

²⁾정회원, (주)희송지오텍

접수일: 2002년 6월 12일

심사 완료일: 2002년 6월 17일

engineers. But, it was an undeniable fact that other researchers except civil engineers did not play an important role in construction of bridges. In the last three to five years, however, a role of geologists, geophysicists, and rock engineers comes to be needed for construction of bridges in special fields of site characterizations. It is the reason that a foundation of piers for a bridge should be investigated carefully because a bridge grows in their length and height.

In this paper, authors would like to introduce a research experience compatible for these cases. The proposed highway contains a lot of tunnels and bridges for the reason as mentioned above. Most of tunnels extend more than 1 km, and some of bridges are constructed at least 100 m higher than a surface in case of places with deep valleys.

This highway is passing through the Cambro-Ordovician Limestone Basin. Actually there are several open-pit mines and quarries in this area. It is known that the limestone in this area contains many natural cavities caused by a movement of a thrust fault and a flow of groundwater. During the excavation of foundations, several natural cavities were found in shallow depth. All the processes for construction were interrupted, and a supplementary site characterization had to be done in detail. Because a guideline for construction of tunnels and bridges was intensified recently in Korea since earthquakes occurred in Turkey and Taipei.

As part of a supplementary site characterization, consequently, several techniques were applied such as a detail reexamination on the existing geological map, a review on the aerial or satellite photographs, and a drilling job for the identification of a rock type. From the geological mapping and drilling, it was found that there were several cavities going with the proposed highway. Thereafter an electrical resistivity prospecting was carried out to investigate the distribution pattern of cavities or fault, and a seismic tomography was also applied to the same site for identification of each layer's pattern and cavity's dimension.

Ultrasonic images for recognizing cavities and discontinuities were obtained in boreholes with a televiewer test, and in-situ wave velocity and in-situ

Poisson's ratio were given from a gamma-log. As investigating the rock mass properties that would be needed for the stability analysis, several tests were performed. A borehole pressure test was carried out for deformation modulus of rock mass, and a hydraulic fracturing test was for in-situ stresses regime. Laboratory tests for general mechanical properties of rock were also done including the direct shear test on a natural joint.

With these data, a numerical simulation was accomplished on before and after reinforcements of rock masses. And finally an appropriate method for reinforcements of rock masses was proposed to secure the stability of the bridge. Fig. 1 shows the entire state of bridge schematically.

2. Geology and Geological Structures

The Cambro-Ordovician limestone is distributed broadly in this area, which is believed to have taken 3 or 4 times folding or faulting actions from the history of geological structures in Korean peninsula. Especially the Moon-Kyung fault, which is one of major faults in Korea, is passing through an adjacent bridge that is located in the southern part of the proposed highway. As shown in Fig. 2, the Moon-Kyung fault is a part of series of large-scale fault, because it connects to the Gak-Dong fault in the direction of NNE.

And also a specified geological map was established together with the proposed lane of this new highway. Fig. 3 shows a geological condition around the proposed road.

The gray solid line means the propose road, and the black solid circle is our target area, the NH 2 bridge. It can be shown from Fig. 3 that limestone and alluvial are widely distributed accompanying the highway, and limestone is mainly distributed around the NH 2 bridge.

As part of a surface geological survey, all discontinuities on outcrops were examined around the NH 2 bridge and concluded to have 4 major joint sets, that is, NS/69°E, N68°W/82°SW, N39°W/86°SW and N52°E/66°SE (Fig. 4).



Fig. 1. Schematic drawings showing cavities and bridge.

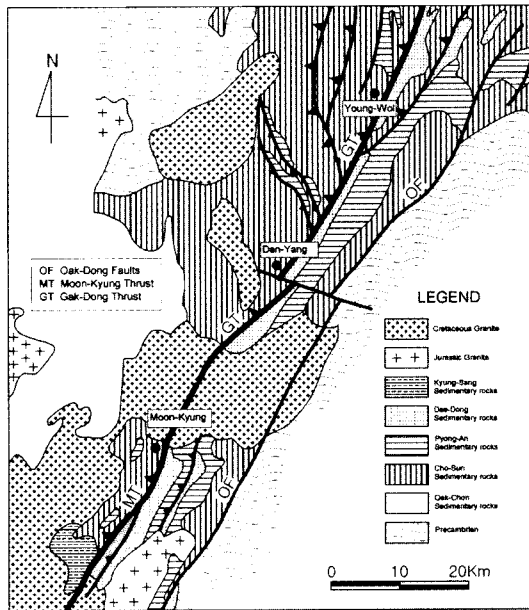


Fig. 2. Large-scale thrust fault developed in NNE and SSW direction.

3. Electric Resistivity Mapping

Boundaries between high and low resistivity can be considered as one of discontinuities, which is generally interpreted as a fault or weak zone in engineering sense. In many cases, these boundaries have a high permeability, and tend to be a flow channel of groundwater. Therefore special treatment will be needed when a construction is passing through these

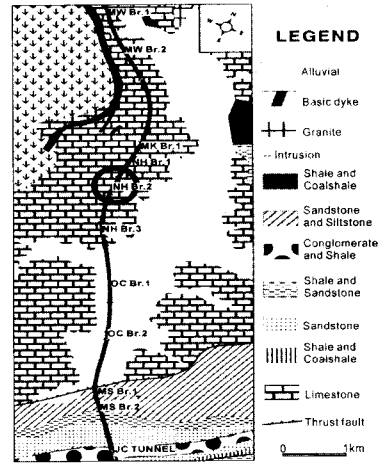


Fig. 3. Geological map around the proposed highway route.

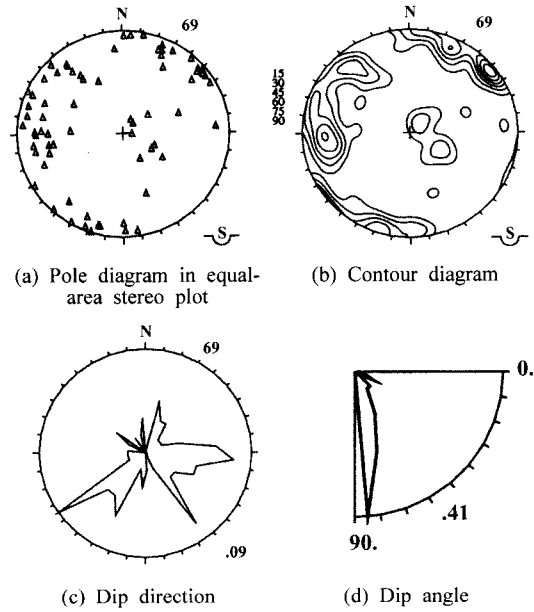


Fig. 4. Discontinuity distribution patterns obtained from outcrops around the NH 2 Bridge.

zones. However it will be dangerous to determine a soundness of rock mass with a resistivity value only, even though it shows generally a high resistivity in a hard rock and a low resistivity in a soft/weak rock.

From the structural geological mapping, it was known that a sub-vertical discontinuity is dominant in this area. Therefore the electric resistivity prospecting method will be effective to find out the distribution pattern of cavities or weak zone.

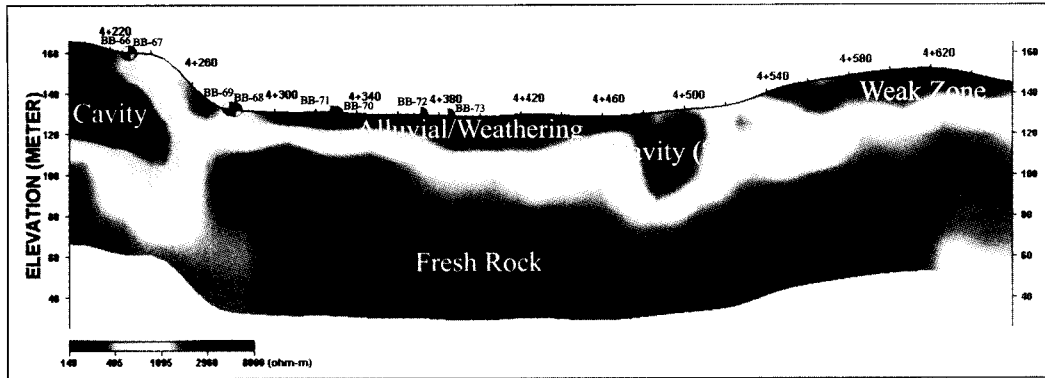


Fig. 5. Electric resistivity profiles in longitudinal direction with dipole-dipole arrays on the NH 2 Bridge.

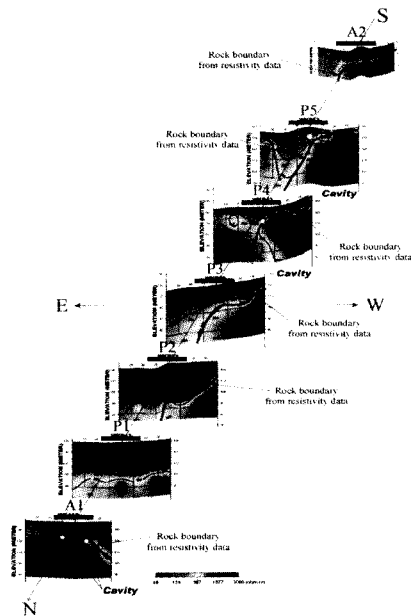


Fig. 6. Multi-profile electric resistivity results from the adjacent bridge foundation. Note that each resistivity profile was obtained through the axial direction of the bridge.

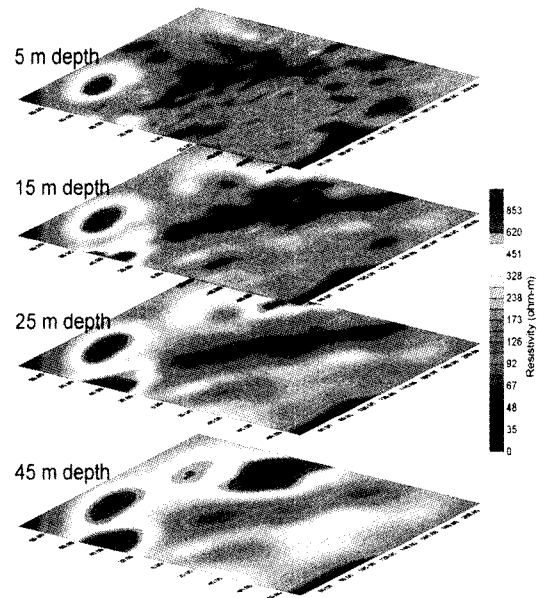


Fig. 7. Three-dimensional electric resistivity results from the adjacent bridge foundation. Note that each horizontal profile was taken with depths.

Fig. 5 shows the electric resistivity profiles on the NH 2 Bridge area. Low resistivity anomaly can be shown beneath the STA.4+220 which position is corresponding to an abutment of the bridge. A drilling job could detect natural cavities at 26 m and 32 m depth. The level of groundwater was 32 meters depth below the surface. This is coinciding well with the fact that cavities are usually developed horizontally along with the groundwater level, that is, a flow path of groundwater. Fig. 6 shows the electric resistivity

profiles on foundations for piers and abutments of the other bridge in the same area. Small white circles in each section mean cavities that were certified by drilling. Sectional profiles of this figure make us to verify the fact that all of the cavities lie on the boundary of a high and a low resistivity. This means that there might be other undiscovered cavities beneath the abutment 1 (A1 profile in Fig. 6) or the pier 3 (P3 profile in Fig. 6), even though it was not verified by drilling. And also it means that natural cavities

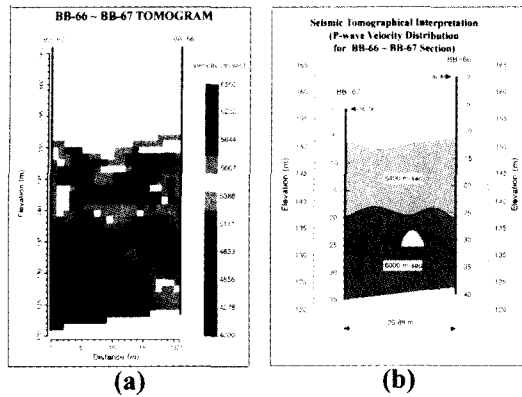


Fig. 8. (a) Seismic velocity distribution pattern for the BB-67~BB-66 section in the NH 2 Bridge site, (b) Schematic engineering model showing petrophysical structures.

could be easily developed in the boundaries between a sound rock and a weak rock. Meanwhile, horizontal distribution patterns of electric resistivity data at a certain depth can be represented well in the three-dimensional technique rather than the two-dimensional. Fig. 7 is one example for the three-dimensional electric resistivity data on the same area to Fig. 6's. A significant spatial anomaly in resistivity data can be revealed. It shows that anomalies are developed diagonally in each horizontal slice, and they are growing downward from 10 m depth.

4. Seismic Tomography and Ultrasonic Images

Seismic tomography was applied to the section between borehole BB-67~BB-66 in the NH 2 Bridge site. The purpose of this test was to identify the formation pattern of each layer as well as the distribution pattern of cavities, which were detected during drilling. This tomogram was compared to the result for the TB-4~TB-3 section that has relatively a good condition of rock mass, because the reference for a seismic velocity in this rock mass was needed for analyzing precisely. Fig. 8 shows the seismic velocity distribution pattern for the BB-67~BB-66 section, which was calculated inversely from the first arrival time of P-wave. In Fig. 8 (a), velocity anomalies were observed partly in the elevation range of 130~

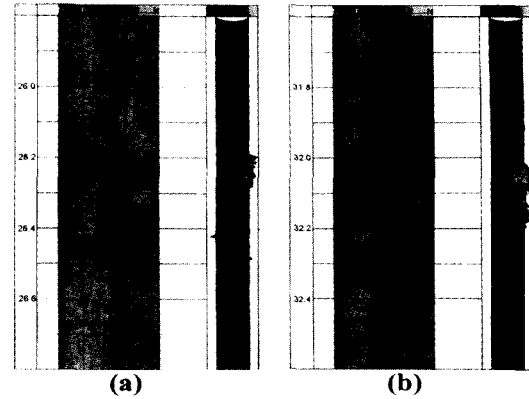


Fig. 9. Ultrasonic images for open joints around the depth of 26 m (a) and 32 m (b).

135 m. This range is corresponding to the depth range of 23~28 m below the surface. And we couldn't fail to notice that these velocity anomalies are isolated with a surrounding homogeneity of velocity. This means that these cavities are isolated and small in scale. So we can figure out layers and cavities schematically as shown in Fig. 8 (b).

An ultrasonic image was obtained also from the borehole BB-66. It was to verify the presence of cavities and to compare the joint sets showing on the borehole wall with those on the outcrop. It was revealed that the rock mass condition for the interval of 24~33 m in depth was relatively poor. Especially, there were large-scale open joints around the depth of 26 m (Fig. 9 (a)) and 32 m (Fig. 9 (b)). And also it was proven that there were two major joint sets, $258^{\circ}/28^{\circ}$ and $279^{\circ}/20^{\circ}$.

A gamma log survey was also performed complementary to the seismic tomography. Namely, the borehole BB-67 was observed by gamma logging tools contrary to the case of the borehole BB-66, in which ultrasonic images were detected. The fractured zone believed to be one of cavities was investigated at the similar depth to ultrasonic images.

And it was known that the P- and S-wave velocities were $5,950 \pm 282$ m/sec and $3,020 \pm 175$ m/sec, respectively. These values are finely corresponding to those of seismic tomography test. Also we could find out the in-situ Poissons ratio is 0.323 ± 0.0304 (Fig. 10).

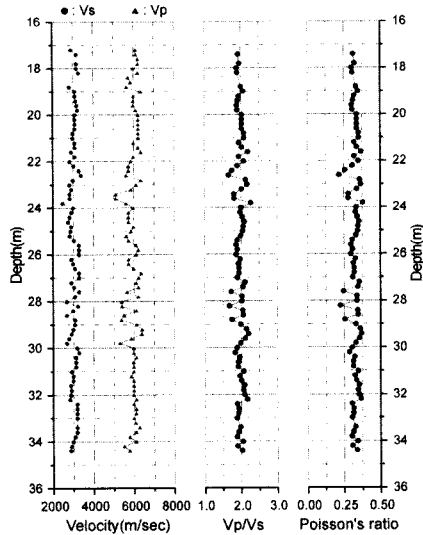


Fig. 10. Gamma-log graphs for Vp, Vs, Vp/Vs, and in-situ Poisson's ratio with depths in the borehole BB-66.

5. Numerical Simulation for Evaluation of Ground Stability

Numerical simulation on the behaviors of ground structures was performed for evaluating the stability of bridges. It was mainly focused on the part where shallow natural cavities are beneath the abutment of the NH 2 Bridge. At this point, as mentioned above, two cavities were found from the geophysical prospecting and confirmed by a drilling. The average size of each was 2 m diameter in the depth of 32 m and

1 m diameter in 26 m depth, respectively. Especially it was found from drilling that these two cavities were connected to each other with a severe open joint. Because when the upper cavity was drilled, the drilling water flowed simultaneously into the lower cavity.

5.1 Outlines

It was certified that there were 4 major joint sets from the geological survey and 2 major joint sets from the statistical analysis on the ultrasonic images. Two of 4 joint sets from the geological survey were corresponding well to joint sets from the ultrasonic images. Consequently only two joint sets were considered in numerical simulations, together with one open joint between two cavities. All of the joint sets were projected on a simulation plane, so the apparent dip angle would be considered for all joints. Universal Distinct Element Code, UDEC versioned 3.0 was used for simulation. It is a kind of DEM program, which can represent fairly the behaviors of all discontinuities as well as rock masses. Three layers were considered in modeling, which was identified through electrical resistivity prospecting as well as seismic tomograms. Physical properties for each layer were adopted by all of test results, namely Poissons ratio from a gamma-log, deformation modulus from a borehole pressure test, cohesion and internal friction angle from a laboratory rock test, and so forth. Fig. 11 shows the procedure for simplifying steps from field conditions to UDEC model. In this model, rock

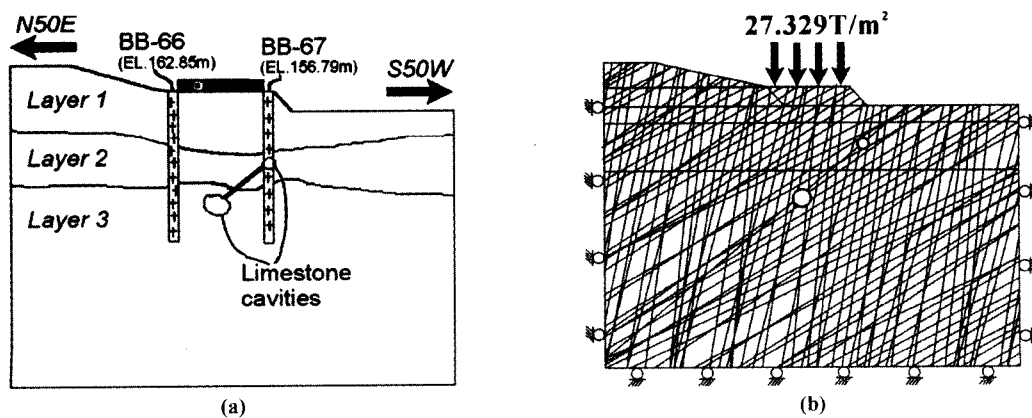


Fig. 11. Schematic drawings for simplifying the procedure from field conditions to numerical models.

Table 1. Physical properties on each layer and joints for a numerical simulation. ρ is density; K is bulk modulus; G is shear modulus; c is cohesive strength; ϕ is internal friction angle; T is tensile strength; JKN is joint normal stiffness; JKS is joint shear stiffness; Jcoh is joint cohesive strength; Jfric is joint friction angle; and Jten is tensile strength of joint.

Rock Properties	Layer 1	Layer 2	Layer 3
ρ (t/m^3)	2.7	2.7	2.7
K (MPa)	7,500	8,300	11,600
G (MPa)	3,500	3,800	5,400
c (MPa)	12	15.0	17
ϕ ($^\circ$)	43	45.0	47.5
T (MPa)	1.0	5.0	9.0
Joint Properties	Joint set 1	Joint set 2	
JKN (MPa/m)	7,080	708	
JKS (MPa/m)	5,880	588	
Jcoh (kPa)	130.0	13	
Jfric ($^\circ$)	23.7	20	
Jten (kPa)	100.0	10	

mass was governed by the Mohr-Coulomb criteria, but all joints obeyed the Coulomb Slip criteria. Finally the distribution pattern for displacements and stresses would be evaluated when the maximum load is applied onto the abutment.

The maximum permissible displacements to bridges are 25 mm in total or 5 mm in difference in Korea. Consequently the stability of a bridge would be classified from the results whether the total or differential displacements are within this limit after loading. The maximum load of 27.329 Ton/m² could be calculated including the dead weight of pier and

slab, the dynamic load from transportations, and the earthquake load.

5.2 Input data and mesh generation

From a drilling job, it was found that the weathered soil distributed up to only 1.5 m depths from the surface, and the others belonged to a hard rock only. So in model, the weathered soil was eliminated and three layers divided the simulation section. Physical properties on each layer are summarized on Table 1.

A fully deformable block would divide each discontinuous block, which forms the whole model. As

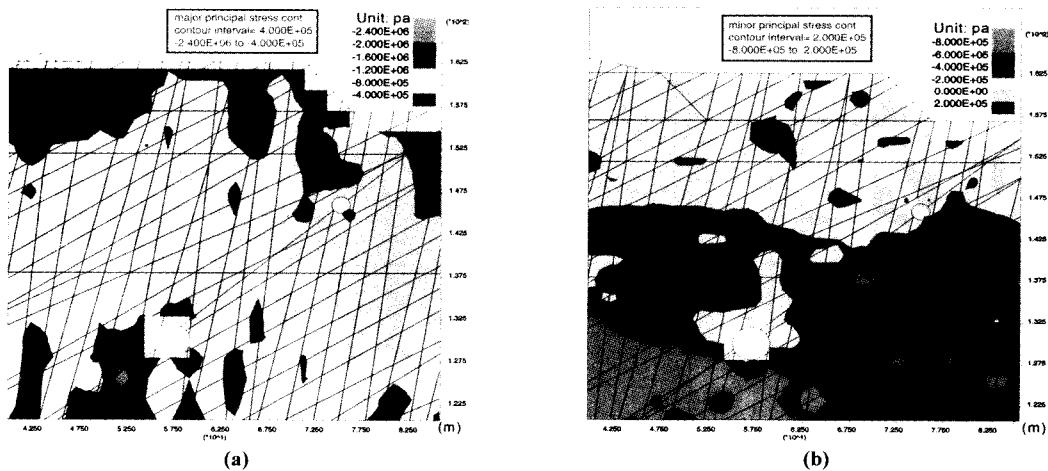


Fig. 12. (a) Maximum principal stress and (b) Minimum principal stress contours developed in rock masses after abutment loading.

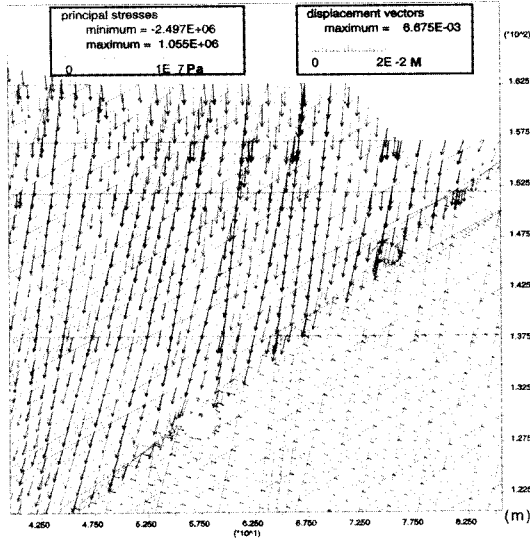


Fig. 13. Displacements and stresses distribution in numerical model.

re zoning blocks fully deformable, each discontinuous block made by joints obey the Mohr-Coulomb plasticity rule.

5.3 Results on the ground stability

Fig. 12 shows the maximum and minimum principal stress distribution in rock masses after loading of 27.329 T/m² onto the abutment. It seems that there is no stress concentration zone in the maximum principal stress contours, but there are stress anomalies along with the joint between the two cavities in the minimum

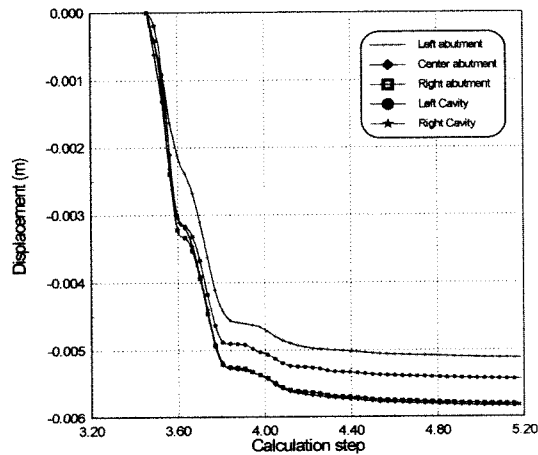


Fig. 14. Displacement history plots around cavities and beneath the abutment.

Table 2. Maximum subsidence occurred in the abutment of the NH 2 Bridge after loading.

beneath the abutment				
Point	Left	Center	Right	Difference
Subsidence (mm)	5.12	5.83	5.80	0.71
above the cavity				
Location	Left-under		Right-above	
Subsidence (mm)	5.43		5.43	

Maximum and differential subsidences are within the permissible limit.

stress contours. It means that there is happening a stress release along this joint.

We can also find out this behavior of each block from Fig. 13, which shows displacement developments and principal stresses. Most of block above this joint are moving downward with a slight angle. Histories of displacements were traced at several points in model as shown in Fig. 14. Finally we could summarize the maximum and differential subsidence as in Table 2.

From Table 2, it seems that two cavities considered in modeling will not have a severe influence on the stability of bridge. However we have to concern that a joint could underestimate possibly the connection between two cavities. Not a joint but a weak or null zone in modeling should represent its connection.

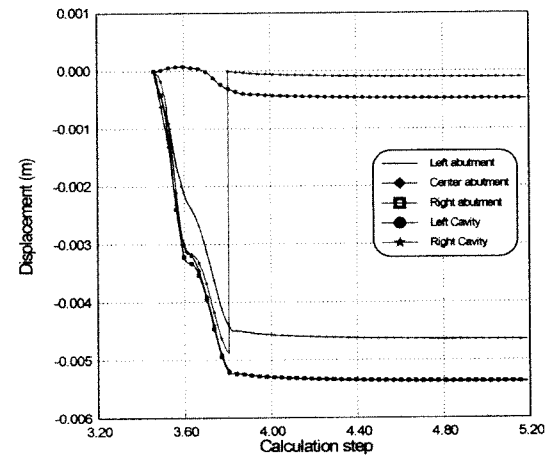


Fig. 15. Displacement history plots around cavities and beneath the abutment after reinforcement.

Table 3. Maximum subsidence occurred in the abutment of the NH 2 Bridge after reinforcement.

beneath the abutment				
Point	Left	Center	Right	Difference
Subsidence (mm)	4.65	5.83	5.36	0.73
above the cavity				
Location	Left-under		Right-above	
Subsidence (mm)	0.48		0.11	

Maximum and differential subsidences are within the permissible limit.

Therefore an additional numerical analysis was decided assuming the reinforcement of cavities.

The FIRM method, which is similar to a general grouting method but is lighter with using a bubble-containing grout, was considered for reinforcement of cavities. Compressive strength of FIRM is known as 6~7 MPa, but 6 MPa was considered in simulation for safety. Therefore its elastic modulus can be calculated by 11.6 GPa, and bulk and shear modulus can be decided by 9.67 GPa and 4.46 GPa, respectively, when Poissons ratio equals 0.3. Fig. 15 and Table 3 show the displacement changes after reinforcement. The generated displacements in several points of the abutment were similar to the case before reinforcement of cavities, but displacements around cavities were decreased extremely. The fact that there is not a big difference in displacement at the abutment but there is a big displacement difference around cavities was owing to exchanges of properties in modeling.

Only exchanging the properties of cavities from null zone to concrete material, namely, simulated the reinforcement of ground. Basically a considerable region including cavities will be strengthened during an actual reinforcement. Consequently we can expect that displacement will decrease surrounding the abutment as well as cavities in a field job.

6. Conclusions

Natural cavities have discovered at shallow depths during constructing the bridge in the Moon-Kyung limestone area. They were considered to be a dangerous element for the safety of structures. Ground condition

including distribution patterns of cavities was reinvestigated with a supplementary field job. A structural geological survey could make a detail geologic map along with a propose lane. And also the formation of layers together with distribution patterns of cavities was evaluated from several geophysical prospecting techniques. Rock mass properties obtained from field tests and laboratory tests were dumped into numerical simulations or extrapolated. UDEC, which is one of DEMs, was chosen for a numerical program, because most of rock mass conditions were fair to good in this region and joints were considered to be a dominant element for the stability of foundation for bridges. From the numerical analysis before and after reinforcement, cavities could be reinforced and displacements could be controlled within the permissible limit for bridges. Moreover larger effects on ground reinforcement were expected in a practical job better than in a simulation job.

This project was a first experience in stability analysis on bridges in limestone area in Korea. If there are some of large natural cavities under foundations of bridges, they could be dangerous elements for the safety of structures. Consequently in case of constructing underground and/or aboveground structures in limestone area or an abandoned mined-out area, a careful site investigation should be preceded with geologists, geophysicists, and rock engineers as a team. In this sense, this project is expected to be a good case study for those similar cases.

Acknowledgements

The site for this research was provided by Doo-Hee Cho in Dae-Han Consultant Co. His help is gratefully acknowledged. Authors also would like to thank Professor Atilla Aydin in Stanford University Rock Fracture Group for discussion and reviewing manuscripts and to Professor David D. Pollard in Stanford University Rock Fracture Group for helpful advice.

References

1. Amadei, B and O. Stephansson, 1997, Rock stress and its measurements, Chapman & Hall, 490p.

2. Amadei, B. and E. Pan, 1992, Gravitational stresses in anisotropic rock masses with inclined strata, *Int. J. Rock Mech. Min. Sci. & Geomech. Abstr.*, 29, 225-236.
3. Bhasin, R. & N. Barton, 1997, A comparison of the Barton-Bandis joint constitutive model with the Mohr-Coulomb model using UDEC, *Environmental and Safety Concerns in Underground Construction*, 413-420.
4. Bieniawski, Z. T., 1978, Determining rock mass deformability: Experience from case histories, *Int. J. Rock Mech. Min. Sci. & Geomech. Abstr.*, 15, 237-247.
5. Choi, S. O., K. C. Han, C. Park, and H. S. Shin, 1996, In-situ stress measurement by hydraulic fracturing for highway tunnel, *Proc. the Korea- Japan Joint Symp. on Rock Engineering*, 217-220.
6. Choi, Sung-Oong & So-Keul Chung, 1999, Stability analysis of a jointed rock slope with the Barton-Bandis Joint Constitutive Model using UDEC, *Journal of Korean Society for Rock Mechanics*, 9(2), 141-148. (in Korean)
7. Doe, T. et. al., 1981, Hydraulic fracturing and over-coring stress measurements in a deep borehole at the Stripa test mine, Sweden, *Proc. 22nd U.S. Symp. on Rock Mech.*, 403-408.
8. Goodman, R. E., 1989, *Introduction to rock mechanics*. 2nd ed., John Wiley & Sons.
9. Haimson, B. C., M. Y. Lee, N. Feknous and P. D. Courval, 1996, Stress measurements at the Site of the SM3 Hydroelectric Scheme near Sept Iles, Quebec, *Int. J. Rock Mech. Min. Sci. & Geomech. Abstr.*, 33(5), 487-497.
10. Hoek, E. and E. T. Brown, 1988, The Hoek-Brown Failure Criterion - a 1988 Update, *Rock Engineering for Underground Excavation, Proc. of 15th Canadian Rock Mechanics Symp.* 31-38.
11. Jaeger, J. C. and N. G. W. Cook, 1976, *Fundamentals of rock mechanics*, 2nd Ed., Chapman and Hall, London.
12. Mohammad, N., D. J. Reddish and L. R. Stace, 1997, The relation between in situ and laboratory rock properties used in numerical modelling, *Int. J. Rock Mech. Min. Sci. & Geomech. Abstr.* 34(2), 289-297.
13. Serafim, J. L. and J. P. Pereira, 1983, Considerations of the geomechanical classification of Bieniawski, *Proc. of Int. Symp. on Engineering Geology and Underground Construction*, Vol. 1, 33-42.
14. Sugawara, K. and Y. Obara, 1993, Measuring rock stress, *Comprehensive Rock Engineering*, Pergamon Press, Vol. 3, 533-552.
15. UDEC manual (ver.3.0) Vol. 1, 2, 3.
16. Yoon, U. S., H. S. Kim and W. S. Choi, 1999, Characteristics of limestone cavities and design for foundation in the Karst: *Proceedings of Korean Society of Geotechnical Engineering*, 399-406 (in Korean).
17. Zoback, M. D. and S. H. Hickman, 1982, In situ study of the physical mechanisms controlling induced seismicity at Monticello Reservoir, South California, *J. Geophys. Res.*, 87, 6959-6974.

최성응



1987년 서울대학교 공과대학 자원공학과, 공학사
 1989년 서울대학교 대학원 자원공학과, 공학석사
 1994년 서울대학교 대학원 자원공학과, 공학박사
 Tel: 042-868-3243
 E-mail: choiso@kigam.re.kr
 choiso@pangea.stanford.EDU
 현재 한국지질자원연구원 탐사개발연구부 선임연구원

김기석



1987년 서울산업대학교 전자공학과, 공학사
 1992년 한양대학교 대학원 전자공학과, 공학석사
 현재 충남대학교 대학원 토목공학과 재학중
 Tel: 02-576-3801 / 042-488-2374
 E-mail: hsgeotek@chollian.net
 현재 (주)희송지오테크 대표이사
